CERN/SPS/80-9/ABT
16 July 1980

EUROPEAN ORGANIZATION FOR NUCLEAR RESEARCH

CERN - SPS

The Design and Prototype Tests of the CERN Antiproton Production Target

R. Bellone, G. del Torre, M. Ross, P. Sievers

Contribution to the Workshop on High Temperature and Energy Density in Target Materials, Fermilab, Batavia, USA

(28-30 April 1980)

1. Introduction

The number of antiprotons ($\bar{p}$) which can be accepted and accumulated in the CERN-$\bar{p}$-storage ring[1] depends strongly, among others, on the parameters of the proton beam incident on the production target and on the target itself. To increase as much as possible the $\bar{p}$-phase plane density, the proton beam must have a small focus and the target material must have a short proton absorption length, i.e. materials of maximum density are required. Moreover, to increase the target efficiency, the target diameter must be matched to the proton beam focus so that the re-absorption of the produced antiprotons in the lateral target material is kept small.

The above requirements, i.e. high intensity, strongly focused proton beams incident on slender targets of heavy material, lead to elevated energy densities and thermal loads in the target material. In the following a target structure is described which attempts to fulfil the above requirements and which still provides sufficient resistance against the beam induced thermal effects.

2. Design parameters

The target will be irradiated with a proton beam of an intensity of 10^{13} protons/pulse and a momentum of 26 GeV/c and a beam diameter of 3 mm at the target location. The duration of each proton burst is 0.4 μs and the burst repetition time is 2.4 s.

The target is made of tungsten which has a density of 19.3 g/cm^3 and a proton absorption length of 10 cm. Since a target length of 11 cm is required, 67% of the incident protons will be absorbed in the material. The target diameter is matched to the beam diameter of 3 mm.

The energy of the incident proton beam is about 41 kJ/burst of which about 2.6 kJ are deposited in the target. This corresponds to an average power dissipation in the target of 1.1 kW.

3. Adiabatic temperature rise per proton pulse

To study the target heating caused by the incident protons and the nucleon-meson cascade induced in the target, calculations of the energy deposition density in tungsten have been made with the Monte Carlo-cascade programme ZYLKAZ[2]. Fig. 1 shows the energy deposition density and the resulting adiabatic temperature rise of at most 1350° C after each proton burst along the target axis. These values indicate that due to excessive thermal stress and thermal shock one must expect yielding or fracture of the target material.

4. Principal target structure

To avoid the desintegration of the target material, the latter must be embedded in a material which is capable of retaining the target fragments, which furthermore can stand the elevated temperatures created around the tungsten and which itself is not destroyed whenever the beam hits accidentally this material. Moreover, the target container must be of low density so that the re-absorption of the antiprotons, emerging from the tungsten target and having to penetrate the container, is as low as possible. Therefore, graphite was selected as material for the target container[3]. This material has an excellent mechanical and thermal resistance at elevated temperatures up to 3000° C and withstands well the heating by the beam[3].

Due to the low density of graphite of about 1.8 g/cm^3 the target efficiency is only slightly decreased. The reduction of the target efficiency as a function of the density of various target support materials is illustrated in Fig. 2.

The tungsten target proper consists of a string of 11 cylinders of 3 mm diameter and 10 mm length each, fitted in a hole of corresponding diameter which is drilled along the core of a graphite cylinder with an outside diameter of 30 mm. At either end, graphite plugs are screwed into the graphite container to seal off the tungsten target. A cut along the axis of the target assembly is shown in Fig. 3. Since both the tungsten and the graphite oxydise at an elevated rate above 500^{o} C in air, the tungsten-graphite assembly must be insulated in an air-tight container. Therefore the graphite is inserted into an aluminium container which is finally closed with thin beryllium or titanium windows at the upstream and the downstream end. Both materials have shown good resistance to the impact of beams of less than 2 mm diameter and 1.5×10^{13} protons/pulse.

5. Steady state and maximum temperature of the target

To evaluate the maximum temperature in the target, the average steady state has to be considered in addition to the adiabatic temperature rise per pulse. The steady state is defined by the overall thermal conductivity from the tungsten through the graphite into the aluminium container, from where the heat is discharged through cooling fins via forced air convection.

The conductivity of the tungsten-graphite transition depends on the surface quality of both parts and on the gap between them. This value is the most difficult to estimate. Measurements between graphite and stainless steel of similar surface quality as the tungsten, including an air gap of 0.05 mm, indicate that a transition conductivity of 0.14 $W/^{o}$ C cm^{2} is easily reached. Applying this value would result in an average temperature difference between the tungsten target and the inner surface of the channel in the graphite of 700^{o} C for an average power dissipation of 1 kW.

The steady state situation has been simulated in an experiment where the tungsten rods in the target assembly were replaced by a cylindrical heating element in which a power of 1 kW was dissipated.

A very good thermal contact between the graphite cylinder and the outer aluminium container is achieved by thermal shrink fitting the latter around the graphite. A temperature jump of about 5^{o} C at this transition was measured.

An efficient air cooling must be applied at the periphery of the aluminium container in order to maintain a low average temperature of this part of the target assembly, since otherwise the thermal contact at the graphite-aluminium transition may be lost due to the large thermal expansion coefficient of aluminium as compared to graphite. With an air speed of 10 m/s around the cooling fins of the aluminium container, an average temperature of about 110^{o} C was achieved in the latter.

As a result of the overall radial thermal conductivity of the assembly the average surface temperature of the tungsten rod will be at most 800^{o} C. Therefore, the temperature along the tungsten core will rise to at most 2150^{o} C after each burst. However, the addition of the average steady state temperature and the maximum temperature rise per proton burst leads again to a somewhat pessimistic estimate.

After a few milliseconds when the Gaussian-like initial temperature distribution over the target cross-section following each burst has become uniform, the target temperature in the core will have dropped by about 700^{o} C. The resulting temperature cycles in the target axis are illustrated in Fig. 4.

6. Prototype target tests with beam

A prototype target, shown in Fig. 5, has been tested at the CERN-PS under the finally envisaged beam conditions. The luminescent screen upstream of the target was viewed with a TV-camera in order to steer the beam properly onto the target.

The target irradiation lasted in total about 12 hours. The interaction rate was monitored with a radiation detector placed downstream of the target. The signal, normalised on the incident proton intensity remained constant within the precision of about 5%. This indicated that no major amount of target material was lost from the initial target volume.

After the remanent activity of the target had cooled down sufficiently[5], an X-ray photo of the assembly was taken and did not indicate any visible damage of the target rods, as shown in Fig. 6.

After further cooling down time the target assembly was machined open so that the target rods could be inspected visually. No gross damage of the tungsten had occurred. However, some rods were fractured along the cylinder axis and the front and end faces were slightly pitted as can be seen in Fig. 7.

It is not yet clear whether these effects were caused by the thermal shock and the excessive thermal stresses, by radiation damage or by the progressive formation of tungsten carbide which occurs at elevated temperatures and which causes a swelling of the material and a reduction in density (ρ(WC) = 15.7 g/cm^3). The latter effect may reduce the target efficiency by about 14%.

7. Material tests at elevated temperatures

In order to evaluate further the formation of tungsten carbide, samples of tungsten rods embedded in graphite were kept at 2000° C over 48 hours in a vacuum furnace[4]. As a result, practically the total amount of tungsten was converted into carbide. A photo of the cross-section of the test sample is shown in Fig. 8.

It is difficult to predict from these results the time over which the tungsten targets are completely converted into carbide under the thermal conditions given by the pulsed proton beam. These tests show, however, that the target efficiency may be somewhat reduced over prolongated irradiation periods.

In case it is discovered in the course of the $\bar{p}$ operation that the formation of tungsten carbide causes significant losses in the $\bar{p}$-yield, rhenium (ρ = 21,04 g/cm^3) will be used as a target material. Heat tests similar to those described above indicate that the latter metal does not form a carbide. However, as shown in Fig. 8, also the Re-rods exhibit microscropic craks and precipitation of graphite at the grain boundaries.

Finally, it could be envisaged to use initially tungsten- or tantal-carbide, which however reduces the target efficiency due to its reduced density. Moreover, Boron or Beryllium based ceramics may be envisaged as target container material, which may be chemically less active. Due to the increased density of ceramics ($\rho \sim 2.3$ g/cm^3), again a reduced target efficiency may result.

8. Conclusion

A quasi thin tungsten target of 3 mm diameter has been designed for an incident proton intensity of 10^{13} protons/pulse at 26 GeV/c and a beam diameter of 3 mm. The target is contained in graphite, which reduces the target efficiency by only about 10%.

Theoretical calculations indicate that energy densities of up to 0.180 kJ/g will occur in the target. This leads to maximum temperatures (steady state plus adiabatical temperature rise/ proton pulse) of 2150^{o} C.

The target has been tested successfully over 12 hours in a beam with the above parameters. The long term behaviour of the designed target will only be experienced in the course of the $\bar{p}$-operation which is due to start in July 1980.

Since the formation of tungsten carbide over prolonged irradiation periods cannot be excluded, some tests have been made with rhenium which is more resistant to chemical reactions with the graphite target container at elevated temperatures. Further options may be the selection of less dense target materials and more dense materials for the target container. This, however, will lead to a reduced target efficiency.

Should the future operation show that the target resists well the beam induced thermal load, a reduction of the target diameter in combination with a correspondingly reduced beam spot may be envisaged. Technically, target diameters of well below 1 mm can be provided with good geometrical precision.

Acknowledgements

We should like to thank L. Hoffmann and his colleagues, in particular D. Simon for the assistance provided during the target tests at the PS. Moreover, the support of M. Höfert /HS and his collaborators for the radiation survey during the target tests is gratefully acknowledged. Finally, we thank J. Adam of CERN/SB and H. Schachner of the Batelle research institute for their collaboration during the metallurgic tests and E. Jones of CERN/PS for his many useful comments and suggestions.

References

1) Design study of a proton-antiproton colliding beam facility, CERN/PS/AA 78-3.

2) Author: J. Ranft, see also H. Schönbacher, CERN-LabII-RA/TM/74-5.

3) Some remarks concerning the $\bar{p}$-production target, P. Sievers, CERN/SPS/ABT/Tech.Note/78-11.

4) Batelle, Centre de Recherche de Genève.

5) Radiation Protection calculations and measurements around the e18-beam in the PS East Experimental Hall, M. Höfert et al., CERN-HS-Divisional Report, 31 October 1979.

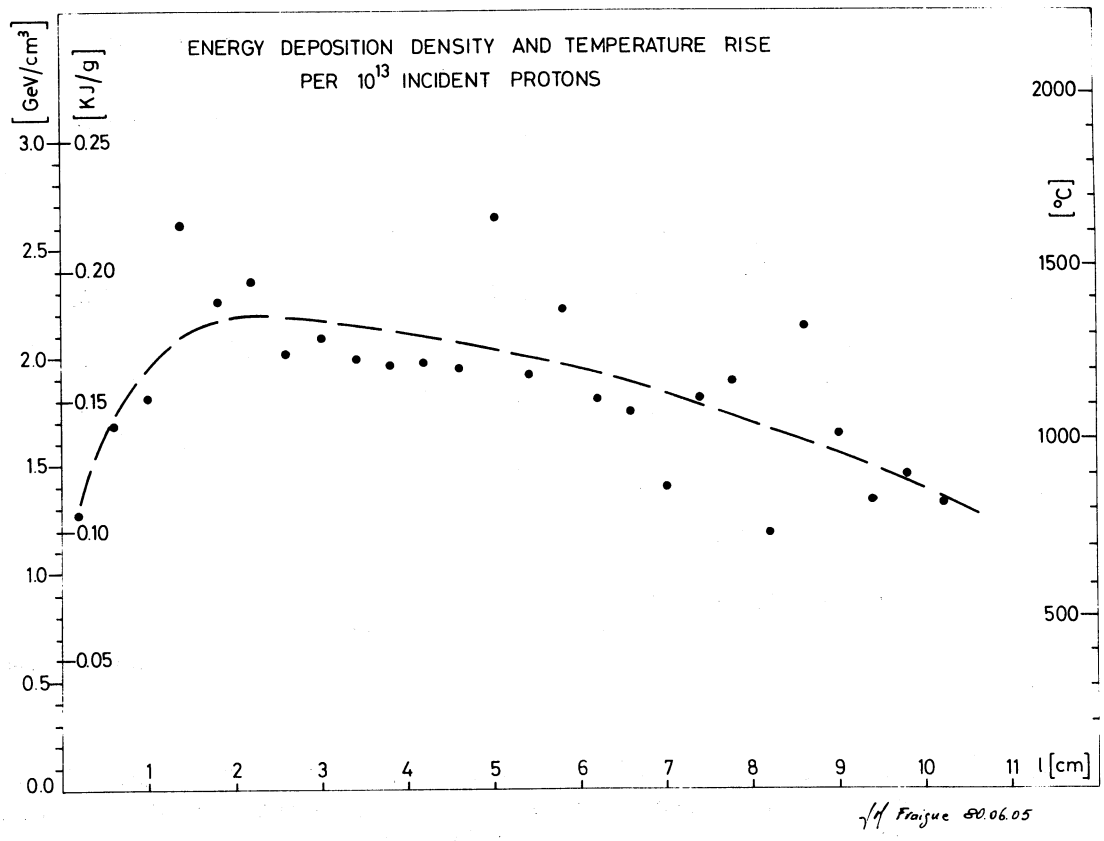

Fig. 1 - The energy deposition density (left hand scale) along the centre of the W-target. The right hand scale gives the resulting temperature rise along the core, where the change of the heat capacity with temperature has been neglected. A beam of 26 GeV/c and a diameter of 3 mm (4 σ of a Gaussian proton density distribution) has been considered.

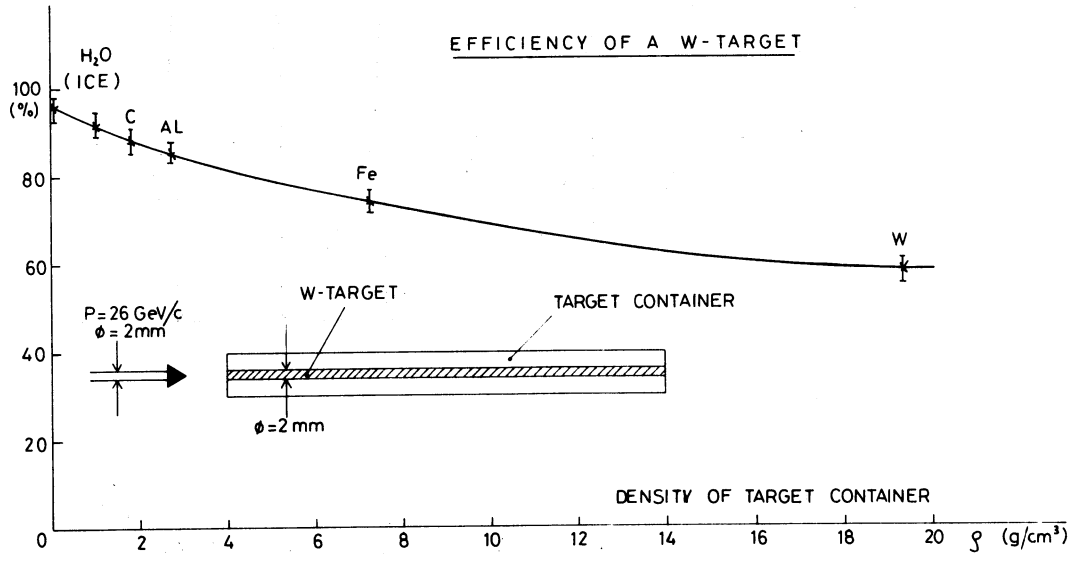

Fig. 2 - Target efficiency (escaping $\bar{p}$'s over created $\bar{p}$'s) of a 2 mm thick and 10 cm long W-target embedded in materials of various densities. Antiprotons of 3.7 GeV/c produced by 26 GeV/c protons within a cone of $\pm$ 50 mrad are considered.

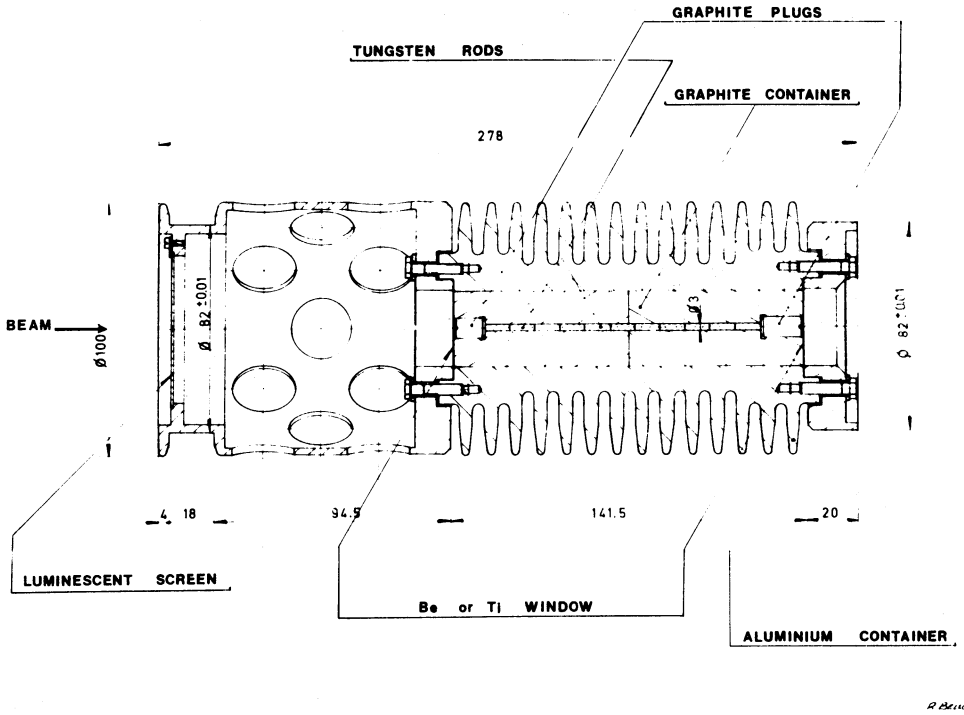

Fig. 3 - Vertical cut through the target assembly. The dimensions are quoted in mm. The perforated aluminium tube upstream of the actual target container offers the possibility to increase the actual target length without a modification of the overall length of the structure and its support (the latter is not shown in this drawing).

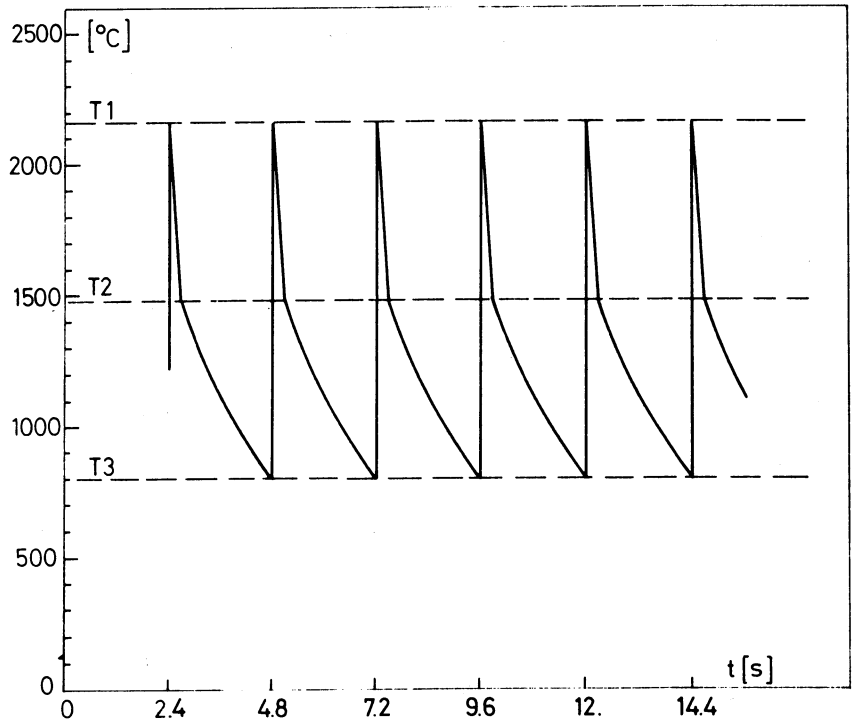

Fig. 4 - Temperature variations in the target centre during each irradiation cycle. The decay from the maximum adiabatic temperature T1 to T2 is due to heat diffusion over the target cross-section (the about Gaussian temperature field becomes uniform) and the decay from T2 to T3 is due to the heat transport towards the cooling fins.

Fig. 5 - Overall view of the target assembly. The aluminium container is anodised black to aid cooling via radiation. The hole in the upstream luminescent screen avoids premature aging and radiation damage of the latter.

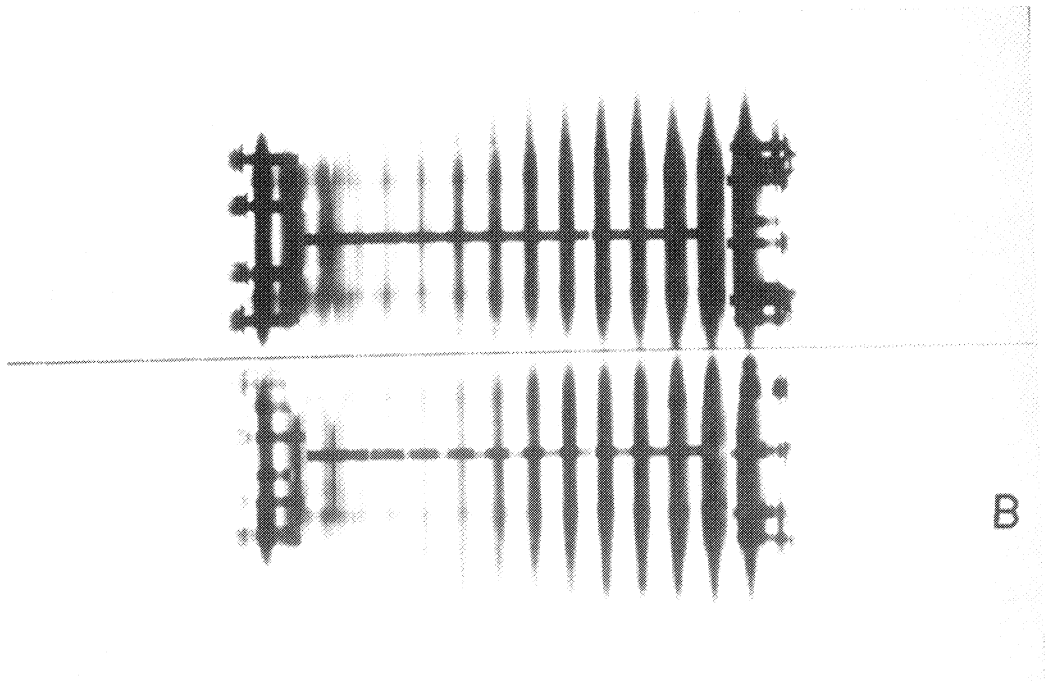

Fig. 6 - X-ray photo of the target ensemble after irradiation.

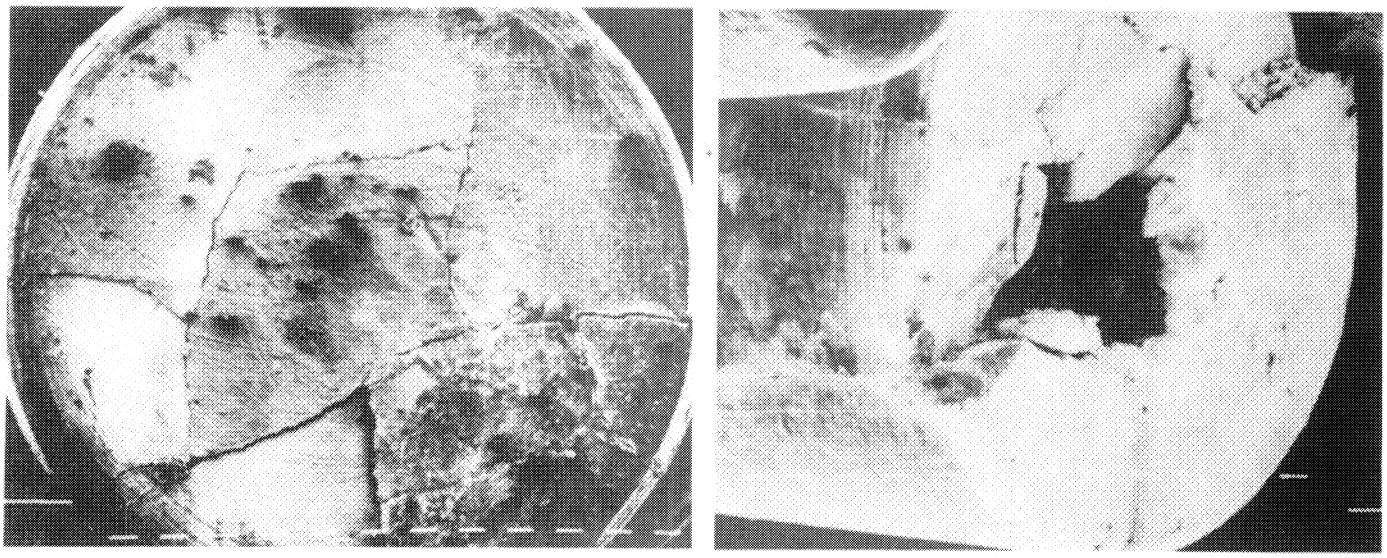

Fig. 7 - Front view of the W-rods after irradiation. The longitudinal craks and a pit of about 1 mm depth can clearly be seen.

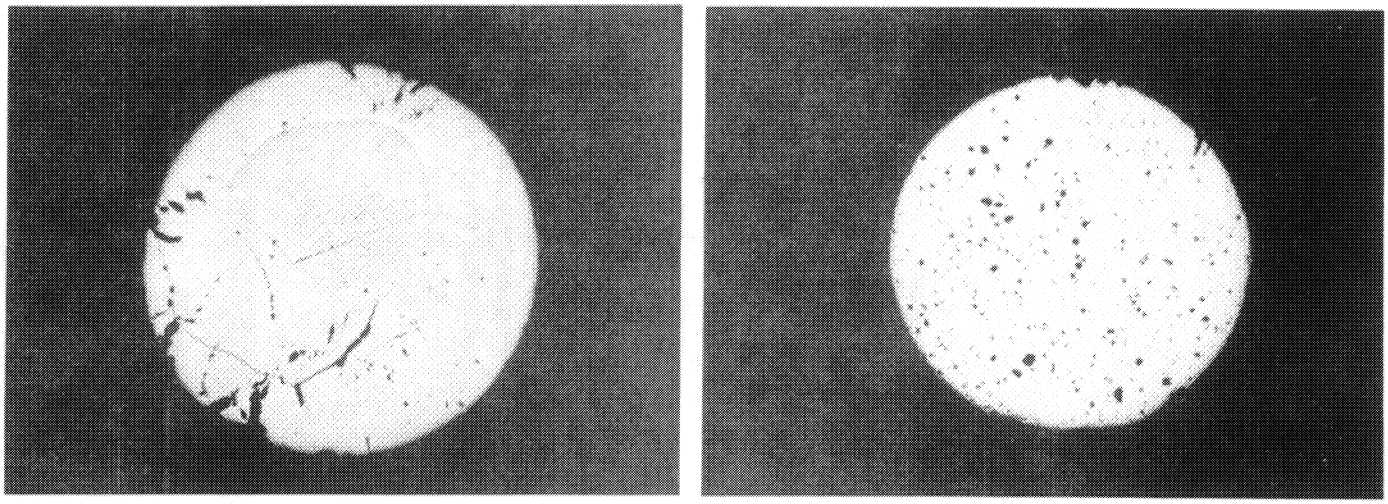

Fig. 8 - Tungsten (left) and rhenium (right) rods after bake-out in graphite at 2000° C over 48 hours. In the tungsten a considerable amount of tungsten carbide was formed. In the otherwise stable rhenium, a slight graphite precipitation occurred at the grain boundaries.